Determination of the Mechanisms Causing and Limiting Separations by Column Crystallization

W. C. GATES, JR., and J. E. POWERS

University of Michigan, Ann Arbor, Michigan

The process of column crystallization at total reflux and steady state was analyzed mathematically and experimentally in order to determine the mechanisms by which separations are achieved and limited. The results of the study indicate that separation is produced by the formation of crystals in the freezing section and by interphase mass-transfer in the adjacent purification section. The separation is mainly limited by axial eddy diffusion in the liquid phase.

Data from three binary chemical systems were used in the study. The first system, *m*-chloronitrobenzene-*m*-bromonitrobenzene, forms a solid solution with a small phase separation (less than 6 wt. %) and was the primary subject of this study. The second system, azobenzene-stilbene, forms a solid solution with a phase separation which exceeds 20 wt. %. The third system, benzene-cyclohexane, has essentially no solid solubility in the range of compositions for which data on separation have been reported (½ to 3 wt. % cyclohexane).

Four mathematical models of column crystallization were developed and compared with experimental data. These models were based on different sets of assumptions as to the mechanisms which control the overall separation. The model which is consistent with experimental data was used to evaluate mass transfer coefficients and effective liquid-phase diffusivities. Diffusivities varied between 1.3 and 4.6 sq. cm./sec., and mass transfer coefficients varied between 0.07 and 0.64 cm./sec. in reasonable agreement with results obtained in studies of liquid-liquid extraction in pulsed columns.

This paper describes a combined theoretical and experimental study of Schildknecht type of column crystallization. The purpose of the study was the determination of the dominant mechanisms acting in this process. This study and determination were warranted by the utility of column crystallization in overcoming the disadvantages previously associated with otherwise attractive crystallization processes and the limited nature of the existing mechanistic or mathematical descriptions of column crystallization.

A brief description of column crystallization is given below to provide a frame of reference for those unfamiliar with this relatively new separation process.

Column crystallization is not like conventional crystallization processes in which a batch of material is uniformly cooled to form crystals which are mechanically separated from the mother liquor. Rather, this process (see Figure 1) is analogous to distillation in a packed column. Two phases pass countercurrently in a purification section along which temperature and concentration gradients are developed and maintained. One of the phases is a continuous reflux liquid, and the other is a disperse solid with little tendency to agglomerate. The solid probably has associated with it a clinging liquid which has a composition different from the continuous liquid.

Mass transfer occurs between the countercurrently moving streams. Thus, the solid and/or any clinging liquid which enter the purification section from the freezing section undergo considerable change in composition before reaching the melting section. In the melting section, energy is supplied in order to convert the solid to a liquid for reflux. Conversely, energy is removed from the freezing section to produce a solid from the liquid which is there.

Like distillation, column crystallization can be operated with continuous feed and removal of products, or at total reflux. In either case, the theoretical attractiveness of crystallization is utilized in a separation process in which solids at their melting point need not be separated from the mother liquor. Quite to the contrary, intimate contact between the solid and liquid is desirable to increase the rates of interphase mass transfer.

The description of interphase mass transfer takes two distinct forms, the form being dependent upon the type of phase diagram which describes the system under consideration. In the first case, the materials form a solid solution as illustrated in Figures 2 and 3 for two of the binary systems considered in this study. In the second case, the materials form a eutectic as is illustrated in Figure 4.

The two descriptions of interphase mass transfer are different because the behavior of the crystals formed from the two types of chemical mixtures is fundamentally different. In the case of solid solutions, the crystals are not pure but contain significant amounts of both components. Such crystals are unstable to changes in temperature. As they move toward the melting section they melt, and under adiabatic conditions (approximated in the purification zone of the column crystallizer), new crystals are formed. The clinging liquid around the melting crystals is displaced into the reflux liquid, and that around the growing crystals probably approaches the reflux liquid in composition. Thus the reflux liquid is effectively the only liquid phase.

Crystals of the eutectic type are without solid solubility so that they are stable to changes in temperature. Thus, as crystals of this type move toward the melting section, there is no driving force for bulk removal of clinging liquid (as differentiated from the case of solid solution), and the reflux and clinging liquids are effectively distinct. The clinging liquid is washed by the reflux liquid which is of considerably higher purity.

More detailed descriptions of column crystallization

W. C. Gates, Jr., is with Texaco, Inc., Beacon, New York.

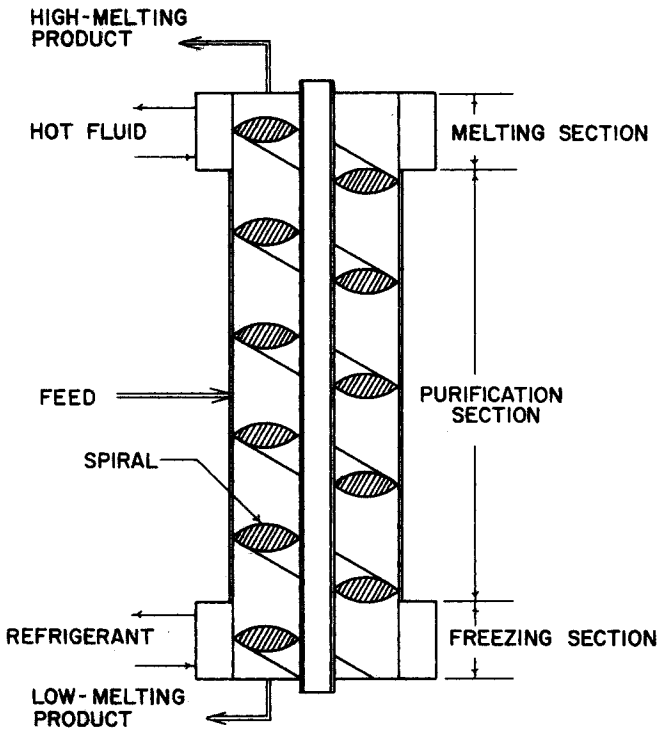

Fig. 1. Sections used in column crystallization.

have been presented (*1, 2, 7*).

SUMMARY OF LITERATURE

Most reports of Schildknecht type of column crystallization (*12* to *14*) are primarily descriptive. Advantages of column crystallization are discussed, and equipment configurations which have been used to carry out the process are illustrated.

Several theoretical analyses have been published (*1* to *5, 7, 11, 17*). In one of the earlier developments, Powers (*11*) recognized the differences between the behavior of solid solutions and eutectic systems but limited his developments by applying an approach similar to that suggested by Furry, Jones, and Onsager (*6*) in the analysis of thermogravitational thermal diffusion columns. His paper included some data which were in qualitative agreement with his analyses, but this early work did not permit the identification of the dominant mechanisms occurring in column crystallization.

Such an identification was recently made by Albertins (*1*) for the system benzene-cyclohexane which forms a eutectic. His basic approach went beyond that used by Powers but was likewise limited in that he considered axial diffusion within the liquid phase to be completely controlling and limited his analyses entirely to systems of the eutectic forming type.

A paper by Henry and Powers (*18*) provides a theoretical and experimental description of continuous rather than batch crystallization for this same chemical system.

MATHEMATICAL MODEL OF COLUMN CRYSTALLIZATION

A single model of column crystallization, one which would consider all possible mechanisms acting in the process and which would apply to all chemical systems, would indeed be complex and difficult to formulate. The approach used in this study was to develop several models, each considering several different mechanisms as dominant, for the case of a solid solution with a small separation factor. The predictions of these models were then compared with experimental data. The analysis used in the only model which was consistent with the data was then extended to apply to two other systems: a solid solution with a large separation factor and a eutectic system. This approach, which considers that the description of the separation achieved in column crystallization is governed mainly by a mass transfer coefficient and by an effective liquid-phase diffusivity, applies equally well to all three systems tested.

Systems which form solid solutions with a small separation factor

The model which describes this type of system is based on the assumption that the changes in composition which occur in the solid phase as it passes toward the melting section are limited (controlled) by the rate at which mass transfer can occur. It is assumed that neither intraphase diffusion nor interphase heat transfer control the observed effects.

The differential description of this model, as it applies to a solid solution, is illustrated in Figure 5. Solid of composition X mass fraction (referring to the component with the lower melting point) moves toward the melting section at a rate L grams per second. Liquid of mass fraction Y moves countercurrently at a rate V grams per second. The composition within each phase is assumed to be uniform in the plane perpendicular to flow. Material is transferred in the axial direction within the liquid by molecular, eddy, and Taylor diffusion at N_C grams per second. Material transfers from the solid to the liquid

Table 1. Summary of Conditions Used in Reported Runs

Run	Nominal charge composition, weight fraction BNB	Crystal rate, g./sec.	Agitation: Rate of oscillation, O/min.	Agitation: Stroke of oscillation, mm.	Agitation: Rate of rotation, rev./min.	Column length, cm.
17	0.50	0.018	31	6.0	29	30.3
18	0.50	0.018	31	6.0	29	25.1
22	0.65	0.031	43	9.0	45	20.0
26	0.65	0.032	43	6.0	48	30.3
29	0.65	0.038	67	4.2	60	30.3
30	0.65	0.033	67	4.2	60	30.3
31	0.65	0.025	67	4.2	60	30.3
33	0.35	0.026	130	2.0	60	30.3
34	0.35	0.017	130	2.0	60	30.3
35	0.35	0.008	130	2.0	60	30.3
13	0.95	0.040	22	4.5	67	30.3

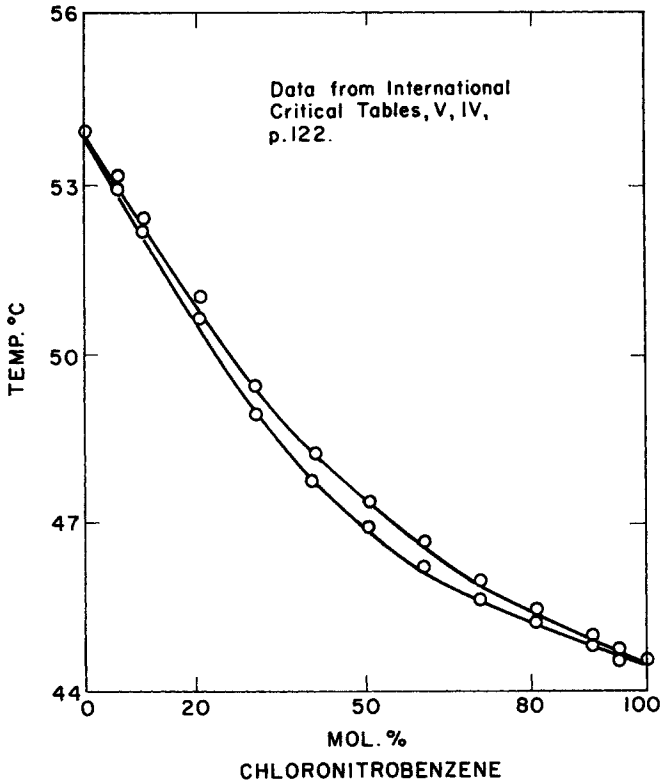

Fig. 2. Phase diagram of *m*-chloronitrobenzene-*m*-bromonitrobenzene.

phase primarily as a result of melting and refreezing at J grams per second. The position z is measured from the freezing section in the direction of crystal flow in centimeters. The rate equations which are assumed to apply are

$$N_C = -\rho DA\eta(dY/dz) \tag{1a}$$

$$J = -\rho KaA\,\Delta z(Y - Y^*) \tag{1b}$$

In accordance with these relations, the total axial dispersion is assumed to follow Fick's Law with an effective diffusivity D square centimeters per second, and mass-transfer is assumed to be proportional to a mass transfer factor Ka seconds^{-1} and to the displacement from equilibrium between phases $(Y - Y^*)$. It is further assumed that D, Ka, the liquid density ρ, the column cross-sectional area A, and the volume fraction of the column occupied by liquid η, as well as the liquid and solid mass flow rates V and L, are independent of position in the column. A detailed discussion concerning these assumptions, with particular reference to the constancy of V and L, is presented elsewhere (7). By incorporating these assumptions, a component mass balance on an element of the liquid gives

$$\rho DA\eta\,(d^2Y/dz^2) + V(dY/dz) - \rho KaA(Y - Y^*) = 0 \tag{2}$$

A total balance and a component balance around one end of the column give Equations (3) for a column operating a total reflux:

$$+V - L = 0 \tag{3a}$$

$$\rho DA\eta\,(dY/dz) + VY - LX = 0 \tag{3b}$$

The solution of Equations (2) and (3) requires another relationship between the dependent variables. Solid liquid-phase equilibrium data serve to relate Y^* and X. In general, the phase equilibrium will be such as to require an analogue or numerical solution to the system of equations [Equations (2), (3), and the equilibrium relation]. However, the phase relation for a system which has a small separation factor is a linear function, Equation (4), over a reasonable range of compositions. A system with such a linear phase relation is *m*-bromonitrobenzene (BNB) and *m*-chloronitrobenzene (CNB) (Figure 2):

$$X = mY^* + b \tag{4}$$

Values for m and b can be determined for the range of composition which applies in a given separation. Combining Equations (2) through (4), and introducing the definitions given by Equation (5), we get Equation (6), the differential equation describing the concentration profile achieved by column crystallization of a solid solution:

$$R_1 \equiv L/\rho DA\eta + \rho KaA/Lm \tag{5a}$$

$$R_2 \equiv Ka/D\eta \tag{5b}$$

$$R_3 \equiv 1/m - 1 \tag{5c}$$

$$d^2Y/dz^2 + R_1\,dY/dz + R_2R_3Y = bR_2/m \tag{6}$$

The solution to Equation (6) has the form given in Equation (7):

$$Y = b/(1 - m) + C_2 \exp(q_2z) + C_3 \exp(q_3z) \tag{7}$$

The constants q must satisfy the characteristic equation, Equation (8):

$$q^2 + R_1q + R_2R_3 = 0 \tag{8}$$

Approximate values of the groupings R_1, R_2, and R_3 can be obtained by estimating values of the parameters comprising the groups. Values of D and K can be approximated from data on liquid extraction in pulsed columns (*8* to *10*, *15*, *16*) (see Table 2). Values of m and ρ are obtained from physical data on the system being investigated. Reasonable values of η, 'a', and the flux L/A

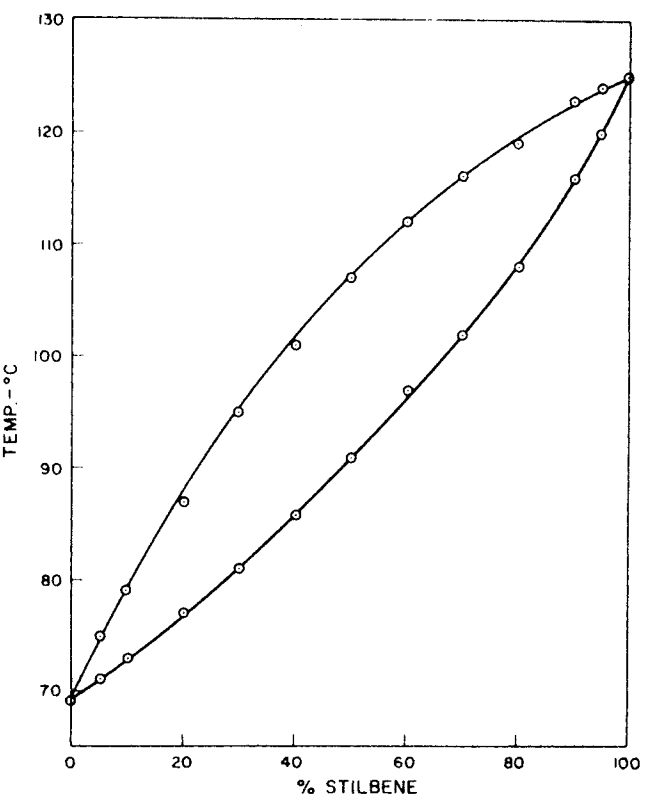

Fig. 3. Phase diagram of azobenzene-stilbene.

have been reported (*1, 2, 7*). By applying these estimated values, it has been established that the particular grouping $4R_2R_3/R_1^2$ was less than 0.1 for all runs made in the course of this investigation (*7*). Under these conditions, the roots of Equation (8), which are both negative, can be closely approximated by Equations (9):

$$q_2 = -R_1 \tag{9a}$$

$$q_3 = -R_2R_3/R_1 \tag{9b}$$

By applying values of appropriate parameters, it can be established that

$$R_1 >> (R_2R_3/R_1) \tag{10}$$

and that

$$R_1h >> 1.0 \tag{11}$$

where h is the total column length. These restrictions apply for most, if not all, practical ranges of operation of column crystallizers of the Schildknecht type.

Consider three special cases involving different relative values of the constants of integration, C_2 and C_3, which are conveniently expressed in terms of the composition of the liquid at $z = 0$, Y_0, and X_0^* calculated by substituting Y_0 into Equation (4). In case I, $C_2 \simeq C_3$; case II, $C_3 = 0$; case III, $C_2 = 0$.

Case I: $C_2 \simeq C_3 = (1/2)(Y_0 - X_0^*)/(1 - m)$. In this case, Equation (7) becomes Equation (12):

$$Y = \frac{b + (1/2)(Y_0 - X_0^*)[\exp(-R_1z) + \exp(-R_2R_3/R_1)z]}{(1 - m)} \tag{12}$$

For the restrictions represented by Equations (10) and (11), Equation (12) predicts a total possible change in concentration, (that is, in a very long column) $\Delta Y_{max} = Y_h - Y_0 = (X_0^* - Y_0)/(1 - m)$. More important, from a point of view of comparison with experimental results, this equation, together with Equations (10) and (11), predicts that one half of the anticipated change will occur in a region very close to $z = 0$. That is, these equations predict practically a discontinuity in liquid-phase concentration at $z = 0$ followed by a much less rapid change in concentration over the rest of the column length.

Case II: $C_3 = 0$. The difference in the values of the two exponential terms in Equation (7) is so great that the second of the exponential terms will dominate over most of the column length unless $C_3 = 0$, that is, unless the second exponential term is suppressed.

TABLE 2. COMPARISON OF EXPERIMENTAL AND LITERATURE VALUES OF DIFFUSIVITY AND MASS TRANSFER COEFFICIENT

Value		Source
Diffusivity, sq.cm./sec.	Mass transfer coefficient, 10^3 cm./sec.	
4.6	0.44	Figure 13
4.2	0.071	Figure 13
3.5	1.9×10^{-4}*	Albertins (*1*)
1.7	0.075	Figure 14
1.5,1.3	0.26,0.64	Figure 14
0.5 to 30		Jones (*8*)
	2 to 5	Lewis (*9*)
	2 to 3	Thorsen and Terjesen (*16*)
0.8 to 2.6		Smoot and Babb (*15*)

* Considered to be incorrectly determined.

If the dominant exponential term in Equation (7) is suppressed, Equation (13) results:

$$Y = \frac{b + (Y_0 - X_0^*)\exp(-R_1z)}{1 - m} \tag{13}$$

Under these restrictions, the liquid-phase composition Y should decrease exponentially and rapidly with respect to z to a constant value, $b/(1 - m)$.

Consider also the influence of crystal rate L on the separation for $C_3 = 0$. According to Equation (5*a*), R_1 will be very large both at small and large values of the crystal flow rate and will pass through a minimum at some intermediate flow rate. As a result, one predicts relatively large separation at both small and large crystal rates with a minimum separation at some intermediate value.

Case III: $C_2 = 0$. For suppression of the first exponential term in Equation (7), Equation (14) results:

$$Y = \frac{b + (Y_0 - X_0^*)\exp[-(R_2R_3/R_1)z]}{1 - m} \tag{14}$$

As for the case $C_3 = 0$, considered previously, this equation predicts an exponential variation in composition with position in the column but does not necessarily predict that Y should approach a constant value at the upper end of the column.

Further simplification of Equation (14) is possible for $(R_2R_3/R_1)h << 1$. Under these conditions, with the further restriction that the equilibrium relation is linear [Equation (4)], Equation (14) reduces to

$$Y = Y_0 - (Y_0 - X_0^*)z/H \tag{15a}$$

where

$$H = mR_1/R_2 = \frac{\rho DA\eta}{L} + \frac{mL}{\rho KaA} \tag{15b}$$

These simplified expressions, Equations (15), predict, subject to the assumptions incorporated in their development, that the composition of the liquid in a column

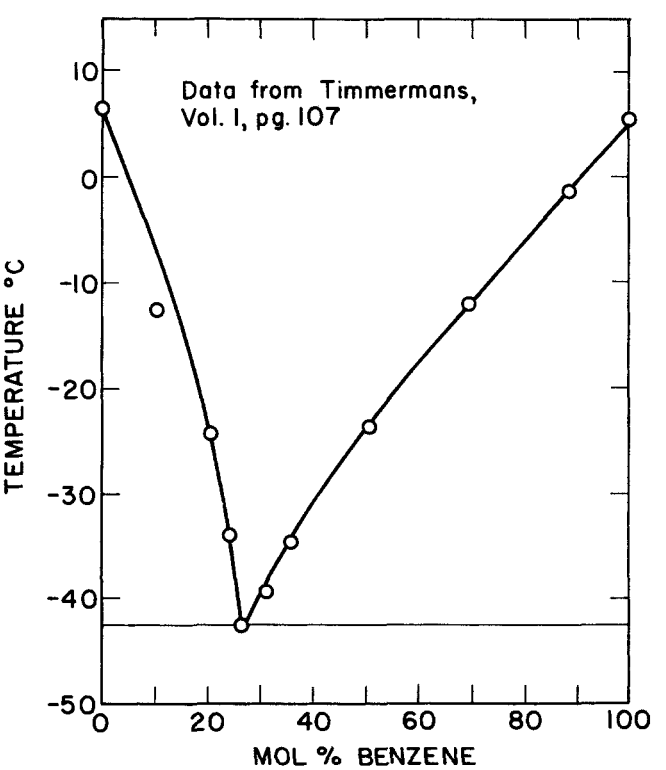

Fig. 4. Phase diagram of cyclohexane-benzene.

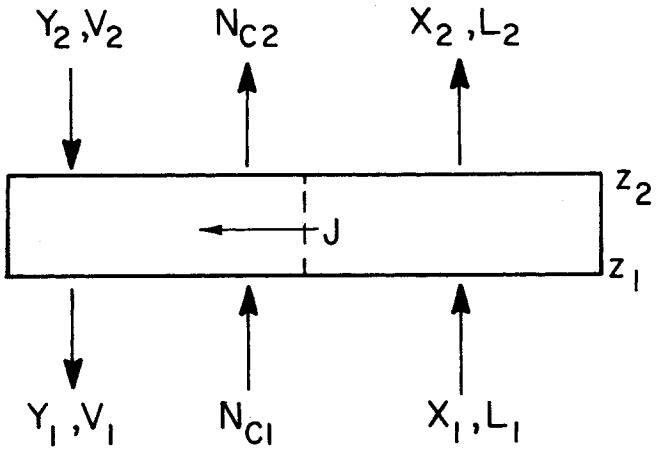

$$N_C = -\rho D \eta A \, (dY/dz)$$

$$J = -\rho K a A \Delta z \, (Y - Y^*)$$

Fig. 5. Differential element in purification section of column crystallizer.

crystallizer will vary linearly with position.

Both Equations (14) with Equation (5) and Equations (15) serve to predict the influence of the crystal rate on the separation. At both very low and very high rates, H is very large, and as a result, the separation is small. The separation passes through a maximum at some intermediate crystal rate.

Other predictions can be made for case III ($C_2 = 0$). For example, it is predicted from Equations (15) that the separation achieved in the column $Y_0 - Y$ is proportional to the extent of the equilibrium separation, as measured by $(Y_0 - X_0^*)$. Thus, as the concentration of the material charged to a column approaches 0 or 100% the concentration gradient should approach zero.

In addition, H, which is evaluated from the concentration gradient, should be a function of composition. The inclusion of m, the slope of the phase relation, Equation (4), in the second term in H is the basis of this prediction.

Systems which form eutectics

In the case of systems which form eutectics and which exhibit little solid solubility, a similar type of analysis to that presented above can be made. Such an analysis (*1, 7*) indicates that the composition profile is exponential, as represented by

$$Y = X_0 + C_1 \exp(-z/H') \qquad (16a)$$

$$H' = D\eta A\rho/L + L\,(1+\alpha)\,\alpha/KaA\rho \qquad (16b)$$

where X_0 is the impurity content of the solid phase which is assumed to be independent of z.

In Equations (16), α is the ratio of the mass of liquid which travels with the crystals to the mass of the crystals themselves. Because α will probably be approximately constant throughout the column, H' is directly analogous to H, which appears in the development of the previous model. The two differ only with respect to m and α. The mass transfer coefficient K refers to the transfer between the reflux liquid and the countercurrently moving clinging liquid.

Equations (16) predict that the difference between the composition in the liquid Y, and a constant X_0 is a semilogarithmic function of position. Thus, plots of $\ln(Y - X_0)$ vs. z should be linear with the slope, $-1/H'$.

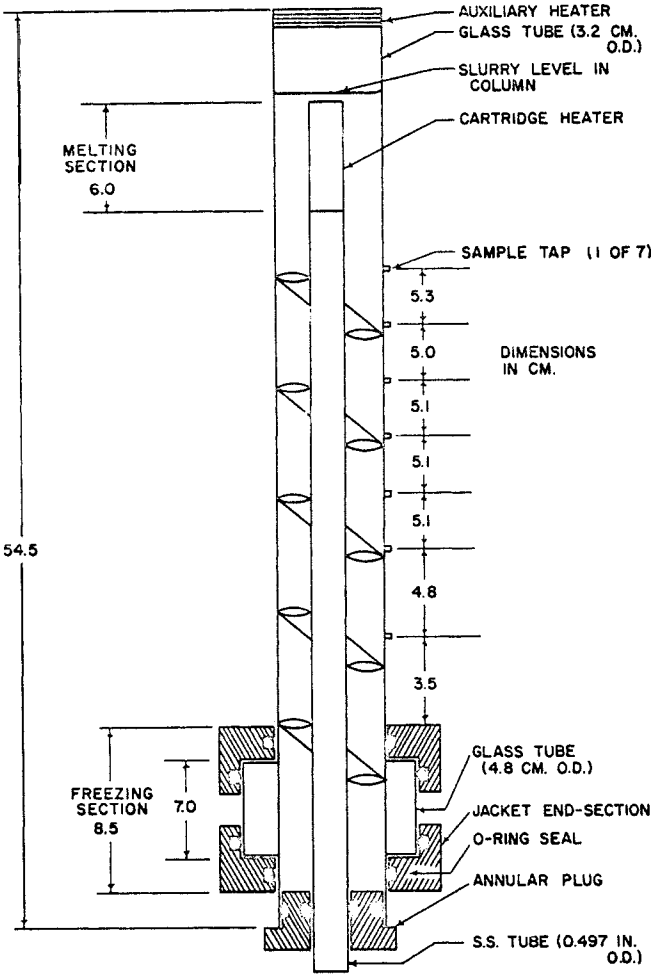

Fig. 6. Diagram of column crystallizer.

It is seen then that in both eutectic type and solid solution systems the value of the factors H and H' is determined by the magnitudes of the crystal rate L, the rate of interphase mass transfer K, and the backmixing effects represented by the effective diffusivity D. From appropriate cross plots of data, values of D and K can be estimated.

Other Models

Two other models, in addition to the one discussed in detail above, were developed and evaluated (*7*). The major predictions resulting from mathematical development of these models were found to be inconsistent with experimental results. Therefore, these developments and the resulting predictions are only very briefly summarized below.

Heat Transfer Limiting Model. A model was developed in which the observed concentration profiles were assumed to be determined in part by the rate of heat transfer between the countercurrently moving solid and liquid phases. This model (which requires computer computation) predicts that the ratio of crystal rate to separation achieved in the column $(L_0/\Delta Y)$ increases linearly with the first power of the crystal rate.

Diffusion In Solid Model. This model was based in part on the assumption that the crystals change composition by molecular diffusion within the solid rather than by melting and recrystallization. This model predicts concentration profiles which are strongly dependent on values of parameters which are subject to check by the results of independent investigations.

EXPERIMENTAL STUDY

Equipment

The equipment used to obtain the data which were used to test the models is illustrated in Fig. 6. This column is very similar to those described by Albertins (*1*) and by others (*11*).

A glass column, 2.60 cm. I.D. by 38 cm. long was used. The freezing section was at the bottom, and the melting section which contained a small electric heater was at the top. The column was equipped with taps which were capped with silicone rubber septums. Samples of reflux liquid could be removed through these septums by using a hypodermic needle and syringe.

A stainless steel spiral, which could be rotated and oscillated at independent rates, passed through the three sections of the column. This spiral acted as an agitator to keep the crystals from agglomerating or settling. This spiral was maintained concentric with the glass by a 1/2 in. diameter stainless steel tube centered in the glass with a nylon plug.

A 4.8-cm. O.D. glass tube, attached to the glass column with nylon rings, formed the freezing section. Water from a constant temperature bath was circulated in the annular space between the glass column and the glass tube.

The operation of the column was made to approximate adiabatic conditions by insulating the glass column with two layers of polyurethane foam, each having a minimum thickness of 5 cm.

Reagents

The system *m*-chloronitrobenzene - *m*-bromonitrobenzene was used in this study. This system, which has a very small separation factor (Figure 2), affords a severe test of the applicability of column crystallization to the separation of systems forming solid solutions. Also, the small separation factor permits several simplifications to be made in the mathematical description. These simplifications make the interpretation of experimental data easier in certain respects.

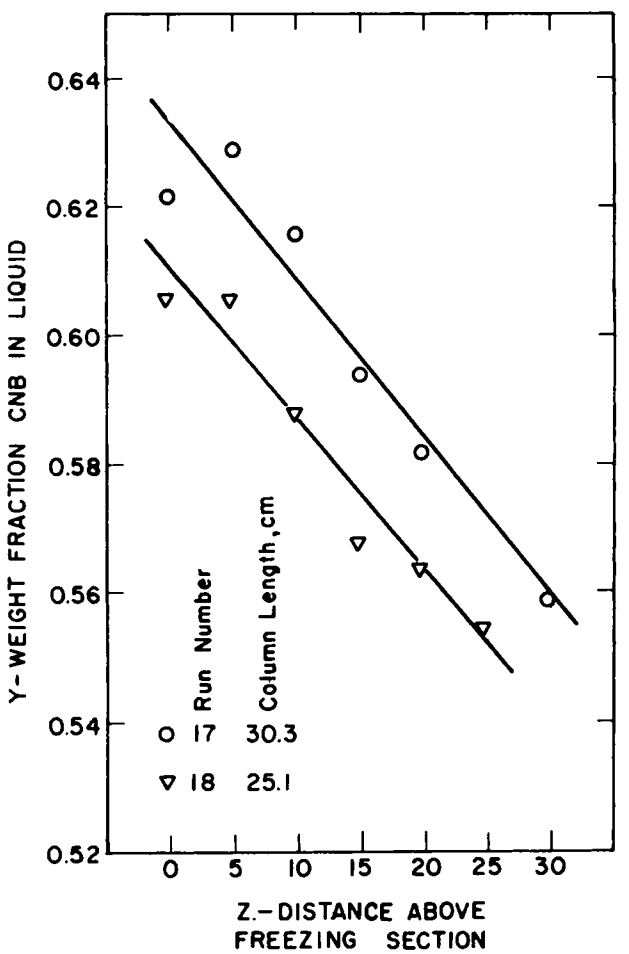

Fig. 7. Influence of column length on concentration profile.

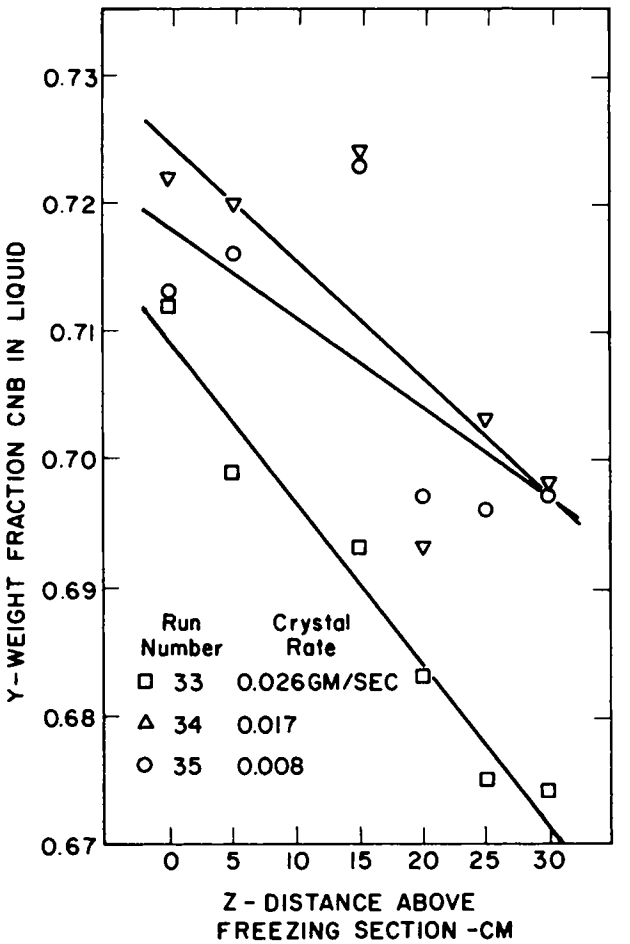

Fig. 8. Influence of crystal rate on concentration profile, low crystal rates.

CNB was used in this study as it was supplied. BNB *from Columbia Organic Chemicals* was recrystallized twice from reagent grade methanol. Total impurities in these two reagents were less than 0.5% as determined by gas chromatography.

Procedure

Liquid of the desired composition was charged to the cleaned and heated column. Warm water at a known temperature below the freezing point of the mixture was circulated through the freezing section to form crystals in the charge. These crystals were agitated by the action of the rotating and oscillating spiral. About 90 min. after the first crystals had been formed, the entire column contained a slurry of crystals and liquid. This slurry appeared to be uniform throughout. No material was fed to the column after the initial charge.

The power input to the melter was adjusted to maintain a constant proportion of crystals. The magnitude of this power input was measured and used to calculate the crystal rate L. About 8 hr. after the first crystals formed, and at least 2 hr. subsequent to any significant adjustment in operating conditions, samples of the liquid in the column were withdrawn, dissolved in reagent grade methyl chloroform, and analyzed by gas chromatography.

To accomplish the purpose of this study, the elucidation of the mechanisms involved in column crystallization, the influence of four operating variables on the experimentally measured separation profile in the column was determined. These variables were the length of the column, the crystal rate through the column, the degree of agitation, and the charge composition.

Results

Experimental results have been presented elsewhere (*7*). Typical results are presented in Figures 7 through 11. The conditions used in the runs reported here are summarized in Table 1.

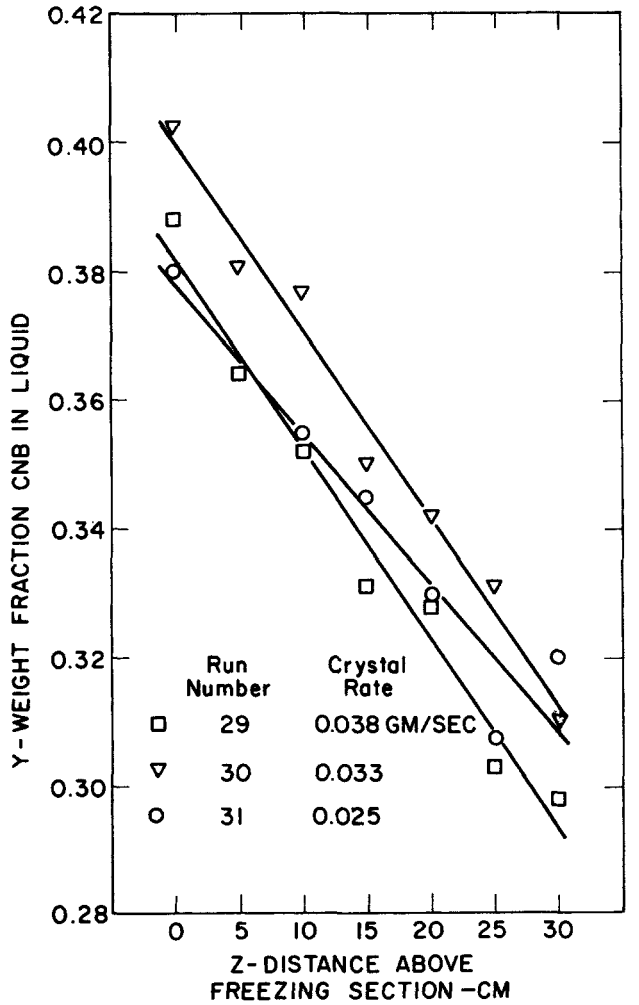

Fig. 9. Influence of crystal rate on concentration profile, high crystal rates.

ANALYSIS OF EXPERIMENTAL DATA

Experimental data were analyzed in an attempt to select a reasonable mathematical model for column crystallization and to determine the factors which play important roles in bringing about and limiting the separation.

Consider Figure 7 in which typical experimental results are presented. Within the limits of accuracy of the experimental determinations, the weight fraction of CNB in the liquid is a linear function of position in the column. There does not appear to be any indication that the concentration decreases rapidly by a significant factor in the region $z = 0$. More significantly, although not shown on Figure 7, samples taken from within the freezing section were consistent with linear extensions of the lines into the freezing section, giving further support to the conclusion that no rapid decrease in composition occurs at $z = 0$. On this basis, it is concluded that C_2 and C_3 are not of similar numerical magnitude (see case I).

The concentration Y does not decrease exponentially to a constant value as predicted by assuming $C_3 = 0$ [case II, Equation (13)]. Therefore, it is concluded that this assumption (which serves to suppress the term which is otherwise dominant throughout most of the column) is not consistent with experimental results. Further support of this conclusion will be presented in a subsequent paragraph.

Equations (15), which result from simplification of the case for $C_2 = 0$ [case III, Equation (14], are consistent with experimental results to the extent that these equations predict that Y is a linear function of z and that the slope $(-1/H)$ is independent of the total column length h. A further consistency check is provided by the fact that the total separations achieved in the two columns of different length operated under otherwise identical conditions are in direct proportion to their respective lengths.

The influence of crystal rate on the separation achieved in the column provides an additional check on the correctness of the alternative assumptions $C_2 = 0$ and $C_3 = 0$. Consider the data presented in Figure 8. Although the data at low crystal rates scatter somewhat, the separation achieved (as indicated quantitatively by the slope of the lines drawn through the individual sets of data) definitely indicate a greater separation at higher crystal rates. This result does not in itself distinguish between the validity of the two assumptions. For $C_3 = 0$, the crystal rates could all be above that of the predicted minimum separation in which case the separation would increase with increase in crystal rate as predicted by Equations (13) and (5a). On the other hand, such an increase is predicted for $C_2 = 0$ by Equations (15) if the separation is less than maximum.

Additional data to clarify this point are presented on Figure 9. These data were obtained at higher crystal rates, and approximately equal separations were obtained at the two higher rates, indicating a leveling off in separation achieved. This result is consistent with the prediction of a maximum according to Equations (15), but is

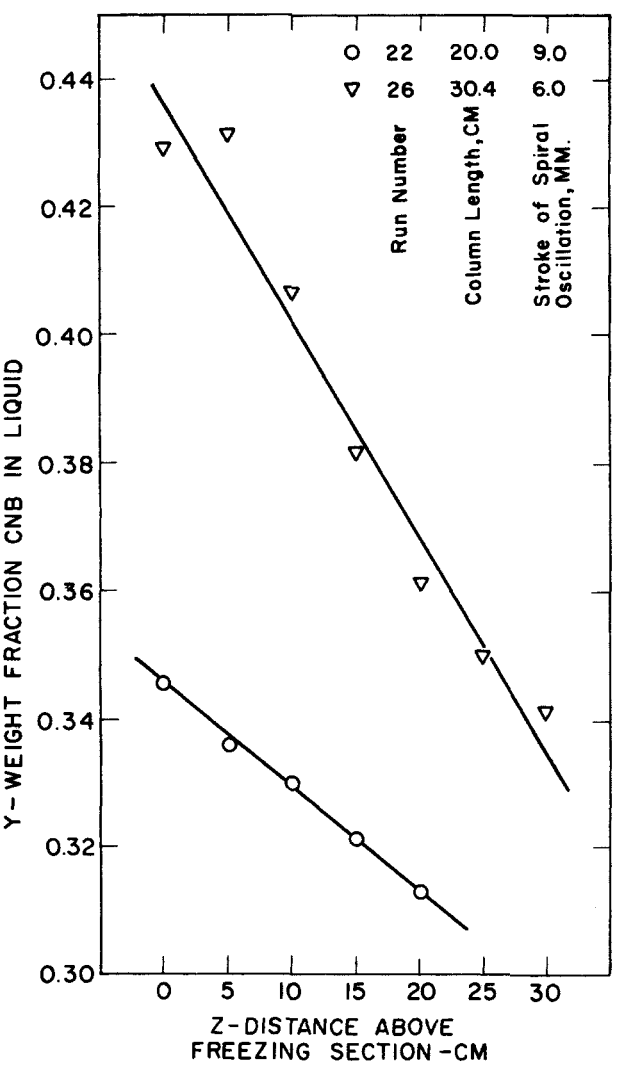

Fig. 10. Effect of stroke amplitude on concentration profile.

clearly inconsistent with Equations (13) and (5*a*). Thus it is concluded that Equation (13), resulting from setting $C_3 = 0$, is invalid.

It is aesthetically pleasing that this is so. In order for Equation (13) to apply in accordance with restrictions as set forth in Equations (10) and (11), it is necessary for C_3 to be equal to zero, or at least for C_3/C_2 to be vanishingly small. However, for Equations (14) [and (15)] to apply, it is only necessary for the ratio C_2/C_3 to be reasonably small, say on the order of 0.1.

The fact that the separation increases to a maximum as the crystal rate increases also serves to establish the dominant factor which influences the separation. According to Equations (15), such an observation is consistent with the fact that axial diffusion (or backmixing) as represented by the group $(\rho DA\eta/L)$ is more important than interphase mass transfer included in the group $(mL/\rho KaA)$. This conclusion is consistent with that obtained by Albertins (*1*).

Results from yet another pair of experiments support this conclusion. These results are presented in Figure 10. Note that as the stroke (and therefore the degree of agitation) is increased, the separation is decreased. It appears reasonable to assume that increasing the intensity of agitation will increase both D and K. An increase in both of these factors will result in a decrease in separation only if axial diffusion is the dominant mechanism. However, the separation will achieve a maximum as indicated in Figure 9 only if the two factors are of equal importance at the higher crystal rates. This possibility was not considered by Albertins. (*1*)

Additional experimental results are consistent with other predictions made from application of Equations (15). Based on the solid-liquid equilibrium data presented as Figure 2, one predicts that the separation achieved in the column should be a maximum near 50 mole % and decrease as the mole fraction approaches 0 or 100. The data presented in Figures 7 to 9 demonstrate that substantial separations were achieved in the range of concentrations from 0.28 to 0.73. As illustrated in Figure 11, very little separation is achieved when material containing only 5 wt. fraction CNB is processed in the column.

This point is further emphasized by the results presented as Figure 12. By rearrangement of Equations (15), one predicts that for operation such that H is constant, a plot of $Y_0 - Y_{30}$ (where Y_{30} refers to CNB concentration in the liquid at $z = 30$ cm.) vs. the equilibrium separation term $Y_0 - X_0^*$ (Figure 12) should yield a straight line with slope $(1/H)$ and zero intercept. Unfortunately, data were not obtained under conditions such that H was constant [see Equation (16) and Table 1]. Thus, Figure 12 provides only qualitative confirmation of the mass transfer limiting model. However, the indicated proportionality which is an eyeball estimate correlates the available data with an average deviation of less than ± 0.02 wt. fraction. These data represent a wide range of charge composition, of crystal rates, and of conditions of agitation, and therefore a wide range in H.

According to Equations (15), H can be determined from the negative slope of a plot of Y vs. z by taking the

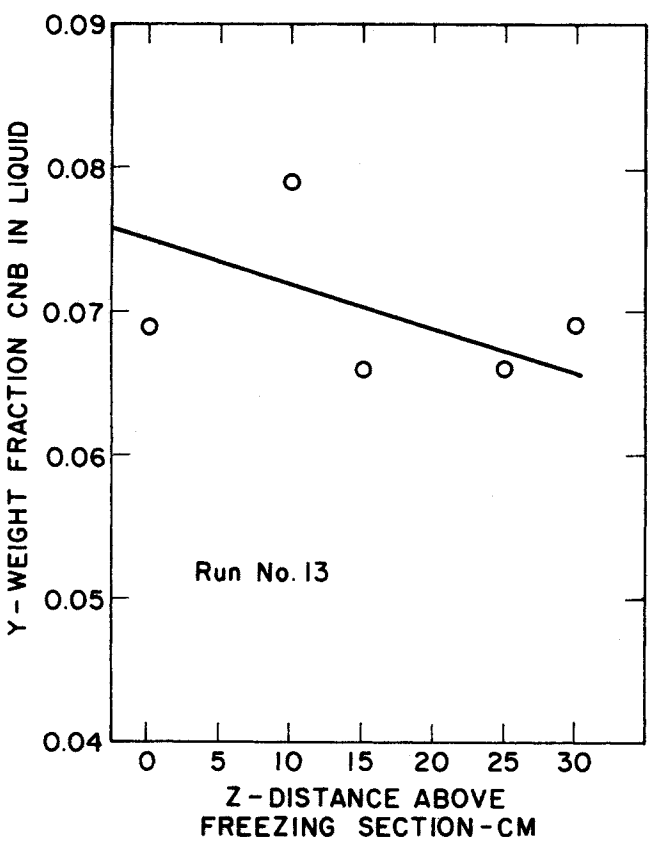

Fig. 11. Concentration profile at low concentration of *m*-chloronitrobenzene.

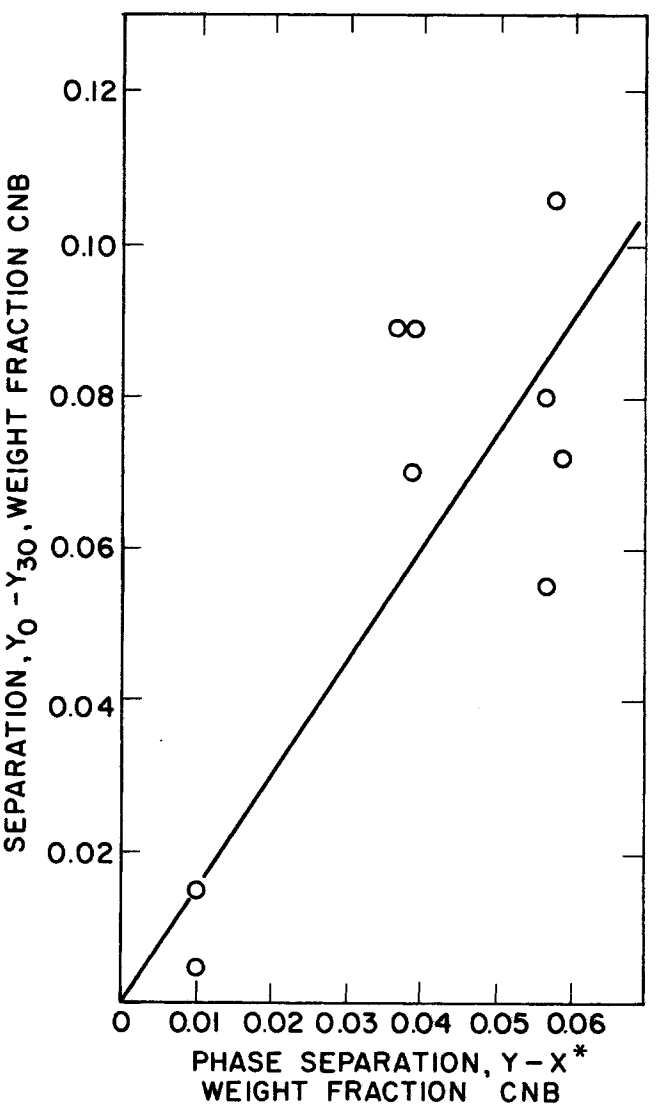

Fig. 12. Dependence of total separation in column crystallizer on difference in equilibrium phase concentrations.

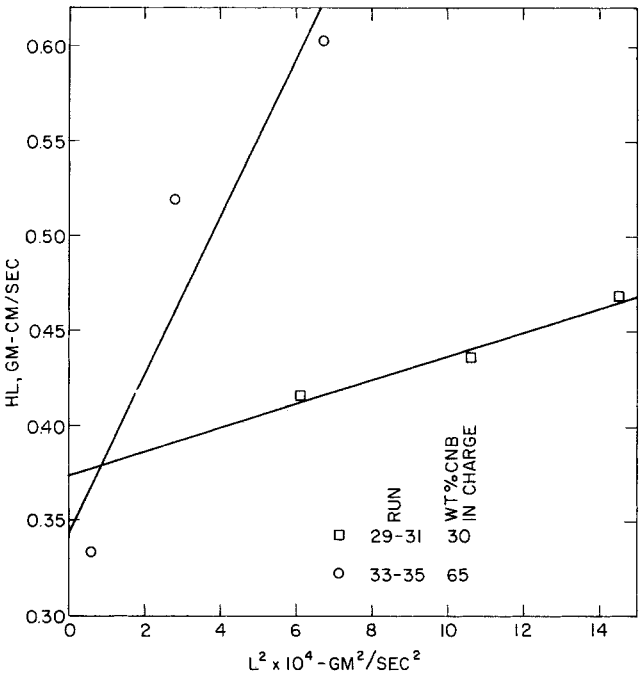

Fig. 13. Determination of diffusivity and mass transfer coefficient for *m*-chloronitrobenzene-*m*-bromonitrobenzene.

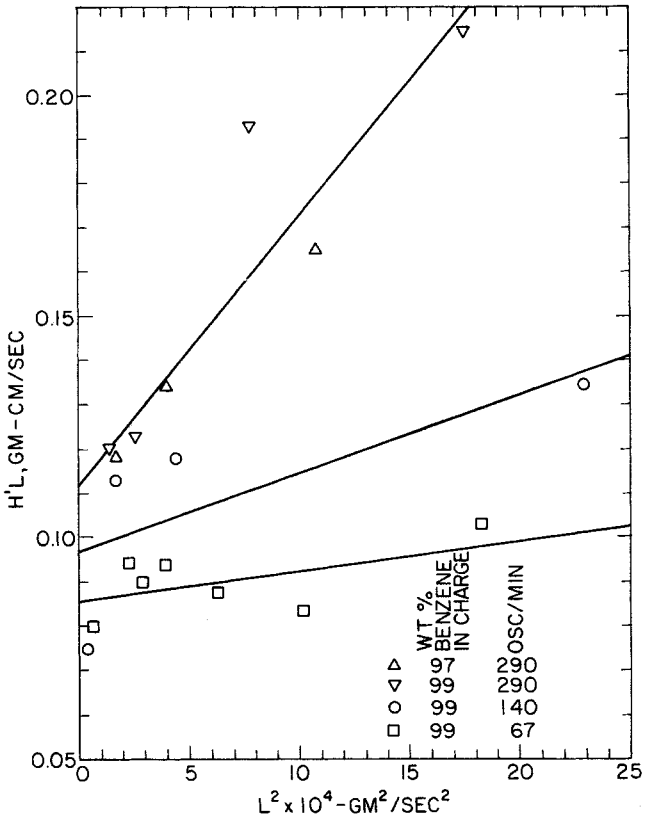

Fig. 14. Determination of diffusivity and mass transfer coefficient for cyclohexane in benzene system.

phase separation factor ($Y_0 - X^*$) into account. Similarly, the data of Albertins (*1*) can be interpreted in accordance with Equation (16*a*) to yield values of H'. Interpretation of the resulting values provides additional information. Examination of the factors H and H' indicates that values of D and K can be determined from appropriate data. Such determinations, in fair agreement with published results for liquid-liquid extraction, are presented below.

If the expression for H (or H') is multiplied by L, then the following linear relations between L^2 and $HL(H'L)$ result:

$$HL = DA\eta\rho + mL^2/KaA\rho \qquad (17a)$$

$$H'L = DA\eta\rho + \alpha(1+\alpha)\,L^2/KaA\rho \qquad (17b)$$

Thus, the intercept and slope of a plot of HL ($H'L$) vs. L^2 can be used to evaluate D and K. Figures 13 and 14 illustrate such plots. The data were fit by a least-squares analysis for objectivity rather than for statistical significance. Although there is scatter, linear fits seem to be adequate. The lines on Figure 13 are based on values of H determined from profiles with CNB and BNB, and those on Figure 14 are based on values of H' reported by Albertins (*1*) [see also (*7*)].

In order to determine values of D and K, values of A, α, η, ρ, and 'a' were estimated for the several operational conditions (*7*). The resultant values of D and K are shown in Table 2.

The calculated diffusivities are self-consistent (similar conditions of operation were used in both studies) and are in fair agreement with published values for diffusivity determined in pulsed-column, liquid-liquid extraction columns (*8* to *10*, *15*, *16*). The values of the mass transfer coefficient seem to be low, however. This disagreement might be the result of different hydrodynamics in liquid-liquid systems and in liquid-solid systems. An effective value for 'a' much lower than the actual 'a' might apply to liquid-solid systems, whereas the effective and actual 'a' are the same in liquid-liquid systems. Use of the actual 'a' where a low effective 'a' should be used would give a low calculation for K.

The necessity of an effective 'a' can be related to the physical phenomena. The crystals probably do not have a uniform distribution of impurity within or along their surface (because they are irregularly shaped). It will be the areas of high impurity which undergo the greatest change in an interval of time. The fraction of the total area occupied by these active centers of impurity should be used in the evaluation of K rather than the total area 'a'.

Although there is considerable scatter in the values of H and H' used to determine the effective diffusivity D and the mass transfer coefficient K (see Figures 13 and 14), the resulting values of D and K in combination with Equations (15) seem adequate to represent the behavior of the columns as illustrated in Figures 15 and 16. Thus, single values of D and K are sufficient to represent the twenty-one basic points of runs 29 to 31, for example, within the limits of accuracy of the determinations.

Additional consideration of the form of Equation (11*b*) indicates that H will decrease with increase of L if the diffusivity term is larger than the mass transfer term. Figures 15 and 16 indicate that diffusion within the liquid phase is, indeed, the dominant mechanism in column crystallization. This result is the same for systems which form solid solutions and those which form eutectics (*7*). Albertins determination of this conclusion took a somewhat different approach. It should be noted that near the limit of operability of the column, diffusive and mass transfer effects appear to be of the same order of importance.

Dependence of *H* on Composition

In the case of solid solutions, the model suggests that H should contain m, the slope of the phase relation. This prediction was not severely tested, but a single test, with a different chemical system used, indicates that the in-

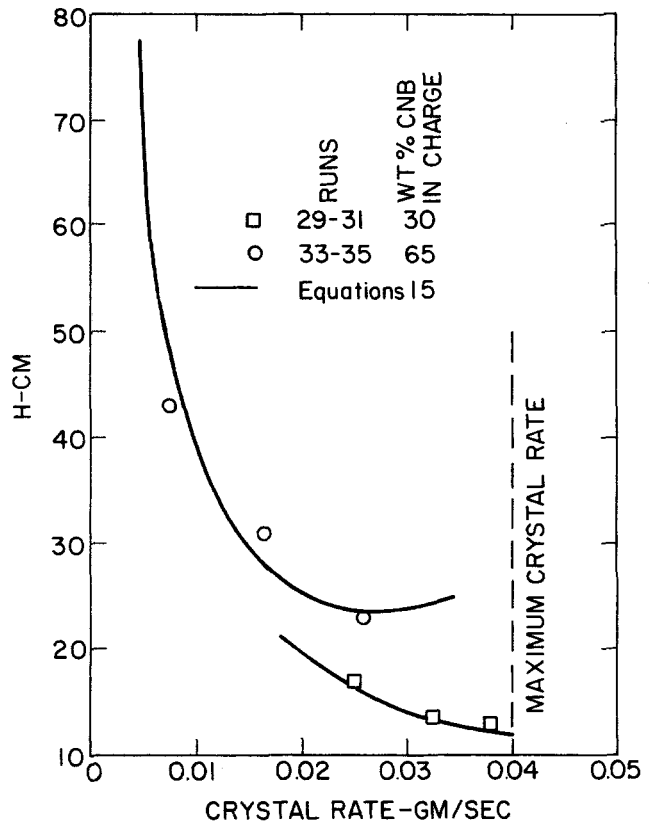

Fig. 15. Effect of crystal rate on separating ability. Comparison of experimental and calculated values for *m*-chloronitrobenzene-*m*-bromonitrobenzene.

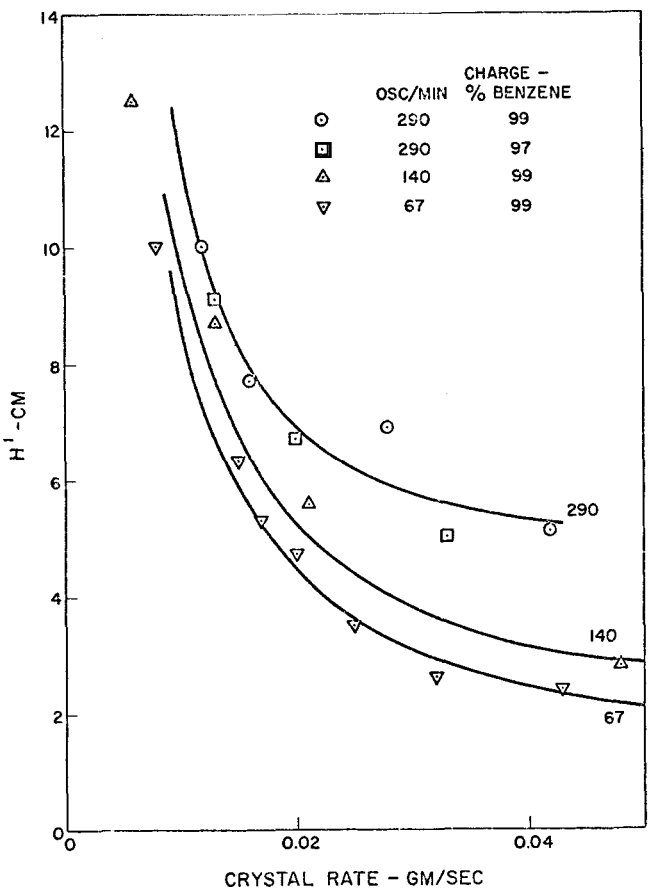

Fig. 16. Effect of crystal rate on column performance. Comparison of experimental and calculated values for the cyclohexane in benzene system.

clusion of m in H is valid [see (7) for details].

In this test, Equations (15), which apply to the case in which m is constant over the length of a column, were applied in a step by step manner to published experimental data for the azobenzene-stilbene system (Figure 3) for which m varies markedly over the column. Much better agreement between the experimental profile and the profile calculated from Equations (15) resulted with variable m than with constant m. This improvement in agreement as the result of a variable m indicates that the inclusion of m in H is valid.

Comparison with other Models

As mentioned under the discussion of theory, two additional models were considered. The heat transfer limiting model predicts that the ratio of crystal rate to separation achieved in the column ($L_0/\Delta Y$) increases linearly with the first power of the crystal rates. Instead, it was found experimentally that this ratio increased as the second power of the crystal rate (7).

The concentration profiles predicted on the basis of composition change within the crystal resulting from intraphase diffusion could only be brought into qualitative agreement with theory, and then only by using values of parameters that are significantly different than those reported in the literature (7).

SUMMARY

This paper reports an experimental and theoretical study in which data from three widely different chemical systems were analyzed by a single approach in order to identify quantitatively the mechanisms acting in column crystallization. The rate controlling step in effecting separations is the mass transfer between the countercurrently passing streams of crystals and liquid. Axial diffusion in the continuous liquid phase limits the separations which can be achieved.

The data on which the above conclusions are based were taken from three sources. Representative data from a system which forms a solid solution with a very small separation factor were obtained during the course if this study. In addition, data previously reported in the literature were analyzed. These include the data of Roessler (12) for a solid solution with an appreciable separation factor and those of Albertins (1) for a system with negligible solid solubility.

ACKNOWLEDGMENT

Valuable assistance was rendered by Professor R. H. Kadlec, Dr. R. Albertins, and J. D. Henry, Jr. Frank Drogosz and L. J. Gates aided in the analytical work. The Upjohn Company donated the drive mechanism for the crystallizer. Financial support for this study was furnished by the Department of Chemical and Metallurgical Engineering of the University of Michigan.

NOTATION

A = cross-sectional area of column, measured perpendicularly to flow of liquid and solid phases, sq.cm.

a = area available for interphase mass transfer per unit volume of column, cm.$^{-1}$

b = intercept of phase relation (4), weight fraction

$C_{\text{subscripted}}$ = constant in general solution to differential equation

D = coefficient of diffusion, sq.cm.

H = grouping of variables, defining the separating power of a column crystallizer operating at spec-

ified conditions, cm.

h = total length of column, cm.

J = rate of interphase mass transfer of CNB, g./sec.

K = coefficient of mass transfer between solid and liquid phases, cm./sec.

L = mass flow of solid, g./sec.

m = slope of phase relation (4), dimensionless

N = diffusional flow of material, g./sec.

q = constant in general solution to differential equation, defined by characteristic equation, $cm.^{-1}$

R = constant defined by Equations (5)

V = mass flow of liquid, g./sec.

X = weight fraction CNB or cyclohexane in solid, g./g.

Y = weight fraction CNB or cyclohexane in liquid, g./g.

z = position in the column, measured from freezing section, cm.

α = ratio of adhering liquid to crystal

Δ = small increment

η = volume fraction, dimensionless

ρ = density, g./cc.

Subscripts

C = CNB

0 = position, $z = 0$

1, 2 = position in column

Superscripts

* = equilibrium value

$'$ = model describing eutectics

LITERATURE CITED

1. Albertins, R., Ph.D. dissertation, Univ. Mich., Ann Arbor (1967).
2. ———, W. C. Gates, and J. E. Powers, in "Fractional Solidification," M. Zief and W. R. Wilcox, ed., Marcel Dekker, New York (1967).
3. Albertins, R., and J. E. Powers, *AIChE J.*, **15**, 554 (1969).
4. Anikin, A. G., *Dokl. Akad. Nauk SSSR*, **151**, No. 5, 1139 (1963).
5. ———, *Russ. J. Phys. Chem.*, **37**, No. 3, 377 (1963).
6. Furry, W. H., R. C. Jones, and L. Onsager, *Phys. Rev.*, **55**, 1083 (1939).
7. Gates, W. C., Ph.D. dissertation, Univ. Mich., Ann Arbor (1967).
8. Jones, S. C., Ph.D. dissertation, Univ. Mich., Ann Arbor (1962).
9. Lewis, J. B., *Chem. Eng. Sci.*, **3**, 248 (1954).
10. Moon, J. S., Ph.D. dissertation, Univ. Calif., Berkeley (1964).
11. Powers, J. E, in "Symposium uber Zonenschmelzen und Kolonnen Kristallisieren," H. Schildknecht, ed., p. 57, Kernforschungszentrum, Karlsruhe, Germany (1963).
12. Roessler, S., Ph.D. dissertation, Univ. Erlangen, Germany (1961).
13. Schildknecht, H., Paper presented at 56 National Meeting, Am. Inst. Chem. Engrs., San Francisco, Calif. (1965).
14. ———, *Anal. Chem.*, **181**, 254 (1961).
15. Smoot, L. D., and A. L. Babb, *Ind. Eng. Chem. Fundamentals*, **1**, 93 (1962).
16. Thorsen, G., and S. G. Terjesen, *Chem. Eng. Sci.*, **17**, 137 (1962).
17. Yagi, S., H. Inove, and H. Sakamoto, *Kagaku Kogaku*, **27**, No. 6, 415 (1963).
18. Henry, J. D., Jr., and J. E. Powers, *AIChE J.*, to be published.

Manuscript received April 22, 1968; revision received November 13, 1968; paper accepted November 14, 1968.

Experimental and Computational Studies of the Dynamics of a Fixed Bed Chemical Reactor

JOSÉ SINAI and A. S. FOSS

University of California, Berkeley, California

Experimental measurements of the temperature response of a fixed bed reactor to sinusoidal disturbances in the feed concentration, temperature, and flow rate show that a simple one-dimensional mathematical model with distributed thermal capacitance satisfactorily describes the dynamic behavior of the reactor for modest excursions about an operating point. The reaction considered is a liquid-phase exothermic reaction whose rate depends on the concentration of two reactants and the temperature.

A computational analysis reveals that the amplitude and phase of the traveling concentration and temperature waves are influenced in a complex manner by the interaction between the two waves. The interaction, which is treated here as interference between traveling waves, is made complex by the difference in the rates of propagation of the temperature and concentration waves and by the variation of their speeds throughout the bed.

Concentration and temperature disturbances are known to propagate through fixed bed chemical reactors in a wavelike manner. While knowledge of the interactions between these traveling waves is central to the conception and design of reactor control systems and to the design of the reactors themselves, there has been only limited exploration of the nature of such phenomena. This paper reports computational and experimental studies of the interaction of traveling sinusoidal concentration and temperature disturbances originating in the reactor feed.

José Sinai is currently with Esso Mathematics & Systems, Inc., Florham Park, New Jersey.